

## 201975: gold grain, Carlow Castle prospect

### (Roebourne Group, Karratha Terrane)

<b>Sample type</b>	Gold grain
<b>Total weight</b>	0.1 g
<b>Sample location</b>	Carlow Castle prospect, about 25 km east-southeast of Karratha
<b>Coordinates</b>	MGA zone 50, 508259E 7698331N
<b>Datum</b>	GDA94
<b>1:250 000 map sheet</b>	ROEBOURNE (SF 50-3)
<b>1:100 000 map sheet</b>	ROEBOURNE (2356)
<b>Tenement</b>	E 47/1797
<b>Collector</b>	Artemis Resources



### Location and sampling

The sample was provided by Artemis Resources in January 2019. It was collected from a sulfide breccia fill in a mafic rock at the Carlow Castle prospect, in the northwest Pilbara region (Artemis Resources, 2019, written comm., 11 January).

### Geological context

The Carlow Castle prospect is located about 1.5 km south of the southern segment of the Regal Thrust, in the Roebourne greenstone belt of the Karratha Terrane and the intrusive 3024–3007 Ma Orpheus Supersuite, northwest Pilbara Craton. The thrust is a regionally significant fault spatially associated with numerous shear-hosted gold and copper deposits in the Roebourne Group and the Nickol River Formation (e.g. Lower Nickol, Weerianna, Carlow Castle, Sing Well; Hickman, 2002, 2016; GSWA, 2020). The local bedrock includes serpentinitized peridotite and dunite of the 3023–3007 Ma Andover Intrusion, surrounded by metamorphosed massive and pillowed basalt, locally fine-grained, spinifex-textured komatiitic basalt of the 3280–3270 Ma Weerianna Basalt, Roebourne Group (Hickman, 2022a,c; GSWA, 2020).

The Carlow Castle prospect is about 1 km east-southeast of the Carlow Castle gold–copper–cobalt deposit, where mineralization occurs in a primary sulfide zone and an overlying supergene-enriched zone. At the Carlow Castle deposit the primary sulfide mineralization is structurally controlled, occurring in sulfide-rich quartz–carbonate veins within a tectonized zone in which there is also extensive chlorite–silica alteration throughout the mafic to ultramafic volcano-sedimentary sequence of the 3280–3261 Ma Ruth Well Formation, Roebourne Group, on the southern side of the Regal Thrust (Fox et al., 2019; Hickman, 2022b, 2016). The Greater Carlow Project has an inferred mineral resource as at 13 October 2022 of 8.74 Mt at 2.5 g/t Au, 0.73% Cu and 0.09% Co (Artemis Resources, 2022).

The nearest regolith landforms are a sheetwash fan unit comprising unconsolidated sand, silt, and clay, local gilgai areas containing expanding clays, and colluvial unit comprising unconsolidated colluvial sand, silt, and gravel, scree and talus, and proximal mass-wasting deposits (GSWA, 2020).

### Methodology

The gold sample was photographed and weighed, and its overall morphology and external features, such as colour, roundness, surface relief, coatings, mineral inclusions and mineralogical assemblages were recorded using visual morphometry. The raw surface of the sample was analysed using scanning electron microscopy with energy dispersive X-ray system (SEM-EDS). The sample was then mounted in epoxy resin, cut and polished and the gold grain microstructure and inclusions were examined using optical and SEM-EDS analyses. Gold microchemistry was determined by laser ablation inductively coupled plasma mass spectrometry (LA-ICP-MS), calibrated against certified gold reference materials (CRM; Murray, 2009). The sample was ablated in triplicate along 0.5 mm-long traverses and average values calculated for elements present in the CRM. The gold surface was repolished after laser ablation, etched with aqua regia, and its internal structure examined using reflected light microscopy and SEM-EDS. Details of this method are described in Hancock and Beardsmore (2020).

### Morphology

The gold grain has dimensions  $5 \times 3 \times 1$  mm and is moderately to well rounded, slightly flattened and with some folded protrusions. Its pitted surface is covered by ferruginous clays (Fig. 1).



**Figure 1. Sample 201975: gold grain, Carlow Castle prospect**

### SEM-EDS analysis of raw surfaces

Much of the surface of the gold grain is scratched and compacted (Fig. 2a), but local domains show a lumpy, blocky polycrystalline mantle with no detectable Ag that has overgrown the strongly damaged surface (Fig. 2b). Cavities in the surface contain ferruginous clays and a few gold nanoparticles.

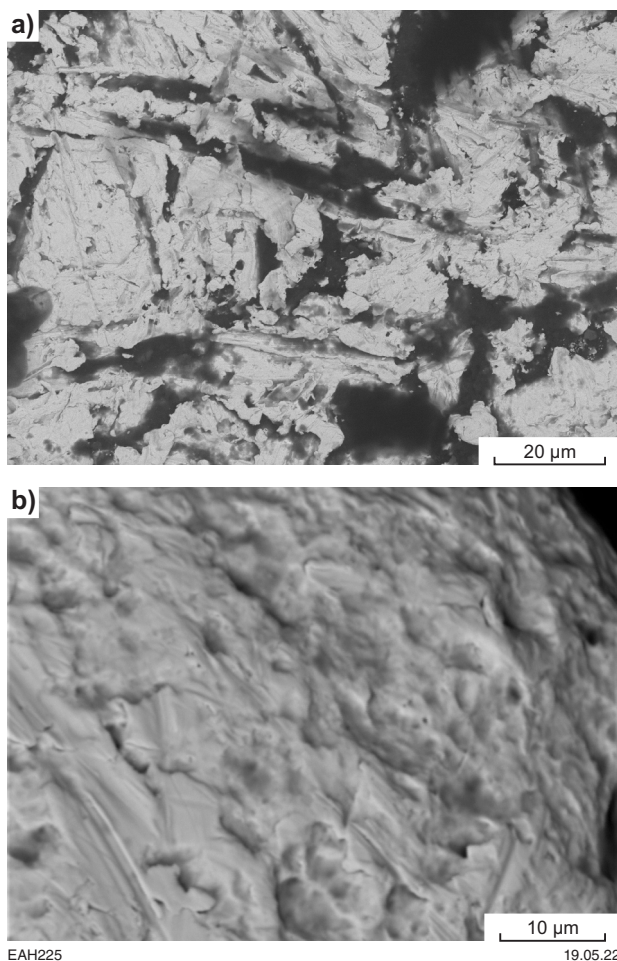


**Figure 2. Backscattered (BSE) and secondary electron (SE) images of sample 201975: gold grain, Carlow Castle prospect: a) BSE; b) SE**

### Optical microscopy of polished surfaces

In section, the grain shows an irregularly scalloped margin, and larger pits and internal cavities indicative of dissolution of gold (Fig. 3a). Quartz and goethite partially to completely fill the larger voids, some of which are round in section, and might have been originally spherical (Fig. 3b).

### SEM-EDS analysis of polished surfaces

The main gold mass contains 4.5 – 5.0% Ag. The internal surfaces of larger cavities commonly have uneven, blocky to stepped microtextures (Fig. 4a), and coatings of Fe-rich kaolin-rich clay containing agglomerations and clusters of pure gold nanoparticles in some cavities (Fig. 4b). Smaller, spherical cavities have smoother internal surfaces with fine-stepped microtexture (Fig. 4c). They contain Ag similar to the main gold mass, and rare nanocrystals of potassium chloride (KCl).

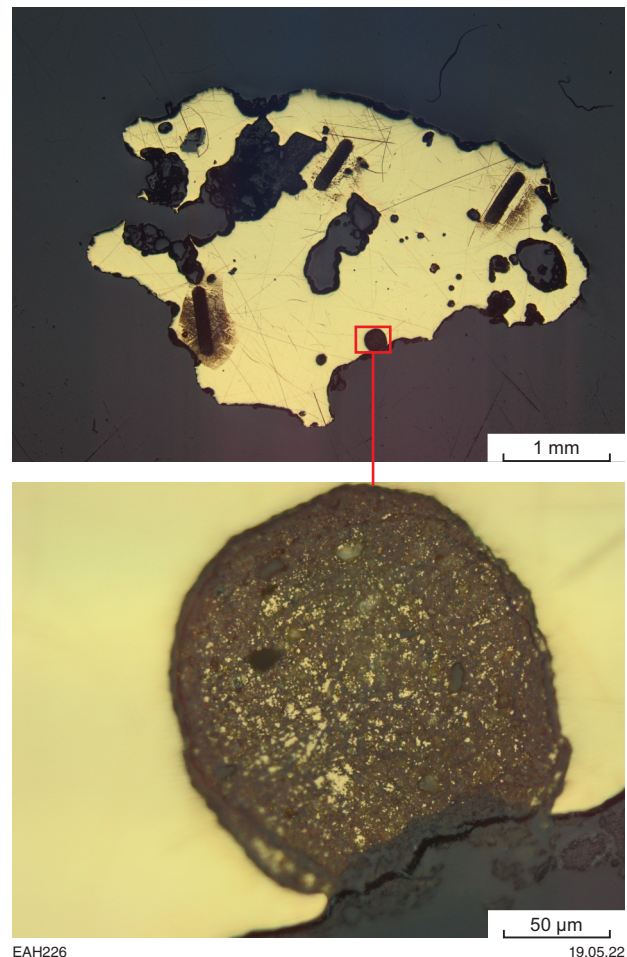


**Figure 3. Reflected-light photomicrographs of polished surface of sample 201975: gold grain, Carlow Castle prospect. Dark, elongate lines are laser ablation tracks produced during LA-ICP-MS analyses**



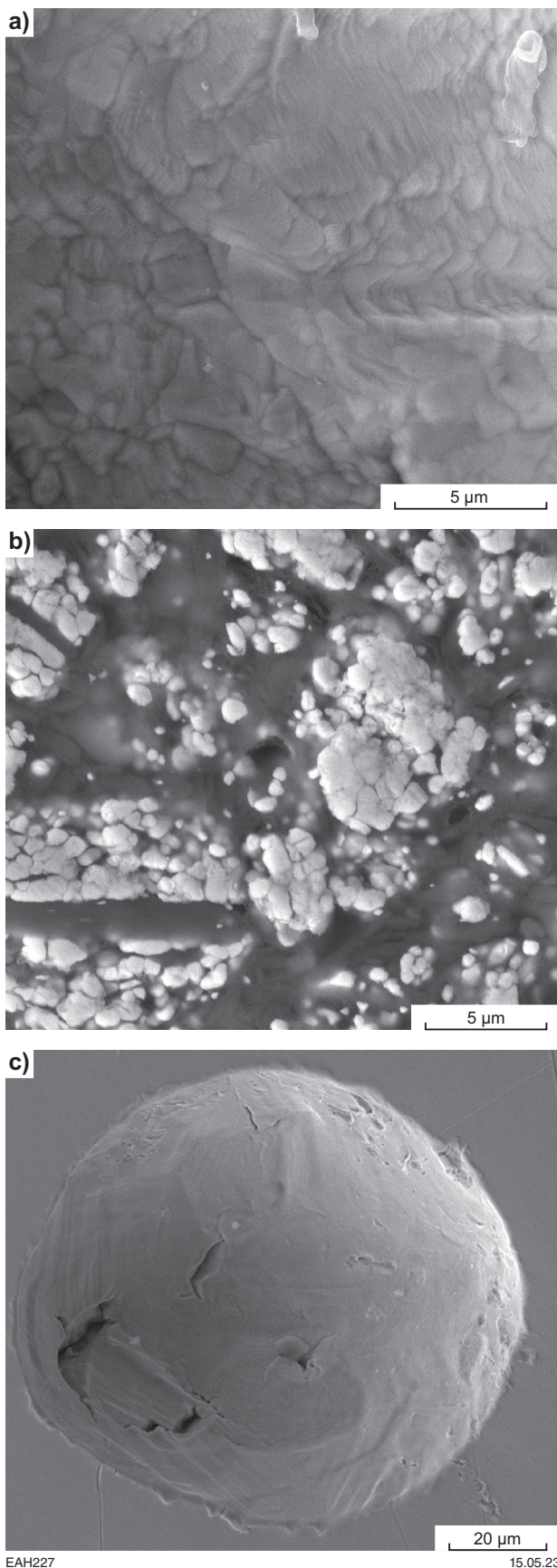


**Figure 4. Secondary electron images of parts of sample 201975: gold grain, Carlow Castle prospect**

## LA-ICP-MS analysis

Analyses consistently detected Ag, Cu and Hg within the gold grain, in concentrations higher than the instrumental detection limit, and probably occurring as limited solid solutions in the gold. Other trace elements were detected only sporadically in low (sub-ppm) concentrations, possibly occurring in micro- and nano-inclusions.

The gold grain contains 3.4 – 3.7% Ag), somewhat lower than the 5% Ag detected using SEM-EDS. Cu content is moderate (313–414 ppm), and Hg is elevated (448–479 ppm) (Table 1). Pd, Mg, Al, Sn, and Sb are also consistently present in the gold grain in low ppm and high ppb levels (Table 2).

**Table 1. LA-ICP-MS data for selected elements in sample 201975: gold grain, Carlow Castle prospect**

Ag (%)	Cu (ppm)	Hg (ppm)	Minor elements
3.4, 3.5, 3.7	313, 393, 414	448, 466, 479	Mg, Pd

## Acid etching

The primary microstructure of the gold is coarsely polycrystalline, with irregular crystal boundaries. There are thin rims of finely recrystallized gold with polysynthetic twinning, which mantling the margins of the grain and some (not spherical) regolith-filled cavities (Fig. 5a,b). A very thin, diffused, paler zone along edges of the grain is probably a polishing artefact (Fig. 5c).

## Interpretation

The primary coarsely crystalline gold grain with low Ag content and no detectable mineral micro-inclusions probably formed from hydrothermal fluids. The spherical cavities within the grain might have been inclusions of this fluid (possibly boiling?) trapped during primary crystallization. The gold grain subsequently experienced partial recrystallization during post-primary deformation, and during erosion and transportation into the regolith. The relatively low Cu content and absence of Co in the gold grain suggests that it is unrelated to the Carlow Castle gold–copper–cobalt deposit. However, consistently elevated Pd implies (re)crystallization of the gold from fluids that have interacted with ultramafic rocks.

**Table 2. LA-ICP-MS compositional data for sample 201975: gold grain, Carlow Castle prospect**

<i>Laser ablation track</i>	<i>Unit</i>	<sup>7</sup> Li	<sup>9</sup> Be	<sup>11</sup> B	<sup>23</sup> Na	<sup>25</sup> Mg	<sup>27</sup> Al	<sup>29</sup> Si	<sup>44</sup> Ca	<sup>45</sup> Sc	<sup>49</sup> Ti	<sup>51</sup> V	<sup>53</sup> Cr	<sup>55</sup> Mn	<sup>57</sup> Fe	<sup>59</sup> Co	<sup>60</sup> Ni	<sup>65</sup> Cu
1	cps					52	120				5			6			8	38713
2	cps					97	89		66		5	3	6			4	6	48651
3	cps					77	98				2	2	34		1	8	10	51314
1	ppm					0.6					0.11						0.08	313
2	ppm					1.2					0.10						0.06	393
3	ppm					0.9					0.03						0.10	414

<i>Laser ablation track</i>	<i>Unit</i>	<sup>66</sup> Zn	<sup>69</sup> Ga	<sup>72</sup> Ge	<sup>75</sup> As	<sup>82</sup> Se	<sup>85</sup> Rb	<sup>88</sup> Sr	<sup>89</sup> Y	<sup>90</sup> Zr	<sup>93</sup> Nb	<sup>98</sup> Mo	<sup>101</sup> Ru	<sup>103</sup> Rh	<sup>108</sup> Pd	<sup>109</sup> Ag	<sup>111</sup> Cd	<sup>115</sup> In
1	cps	2		3	9		5	3			7			4	152	7106761	8	
2	cps	11						5	1		6		1		176	7576498	12	
3	cps	19		4			7	6		3	16				169	7246890	8	1
1	ppm	0.02			0.10									0.01	1.2	34482		
2	ppm	0.13													1.3	36761		
3	ppm	0.22													1.3	35162		

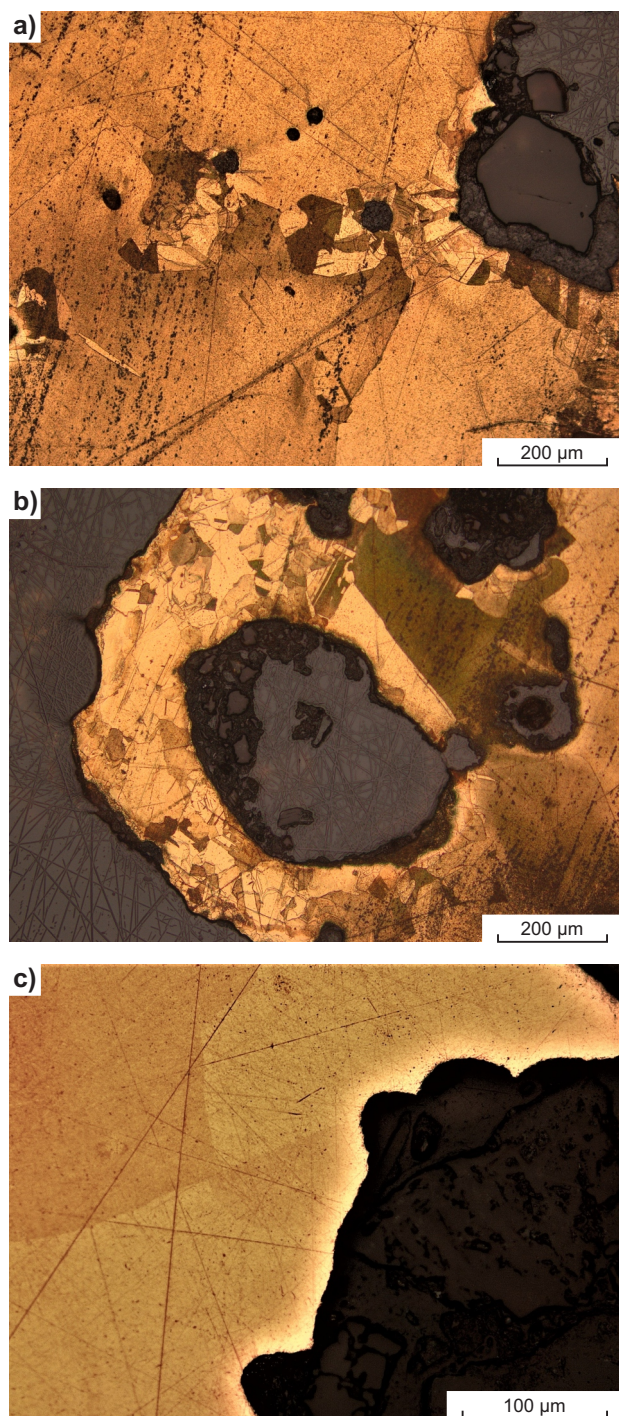
  

<i>Laser ablation track</i>	<i>Unit</i>	<sup>120</sup> Sn	<sup>121</sup> Sb	<sup>126</sup> Te	<sup>133</sup> Cs	<sup>138</sup> Ba	<sup>139</sup> La	<sup>140</sup> Ce	<sup>141</sup> Pr	<sup>145</sup> Nd	<sup>151</sup> Eu	<sup>157</sup> Gd	<sup>159</sup> Tb	<sup>162</sup> Dy	<sup>165</sup> Ho	<sup>167</sup> Er	<sup>169</sup> Tm	<sup>172</sup> Yb
1	cps	90	151	3		2				2		2			1			
2	cps	125	32	4		2						1	1					
3	cps	126	19	2	3	5		1										
1	ppm	0.40	0.59	0.05														
2	ppm	0.56	0.12	0.06														
3	ppm	0.57	0.07	0.03														

<i>Laser ablation track</i>	<i>Unit</i>	<sup>175</sup> Lu	<sup>178</sup> Hf	<sup>181</sup> Ta	<sup>182</sup> W	<sup>186</sup> Re	<sup>189</sup> Os	<sup>193</sup> Ir	<sup>195</sup> Pt	<sup>202</sup> Hg	<sup>205</sup> Tl	<sup>208</sup> Pb	<sup>209</sup> Bi	<sup>232</sup> Th	<sup>238</sup> U
1	cps									129996			2		3
2	cps						2		1	138814		9	3	2	
3	cps			1				3	1	135031	2	9	2		2
1	ppm									448			0.004		
2	ppm								0.01	479		0.03	0.006		
3	ppm								0.01	466		0.03	0.004		

Notes: cps, count per second; ppm, parts per million



**Figure 5.** Reflected-light photomicrographs, after repolishing and acid etching, of parts of sample 201975: gold grain, Carlow Castle prospect

## References

- Artemis Resources 2022, High-Grade Gold Copper Cobalt Inferred Mineral Resource Lays Foundation for a Robust Greater Carlow Project (media release): Australian Securities Exchange (ASX), released 13 October 2022, 41p.
- Fox, DCM, Spinks, SC, Pearce, MA, Barham, M, Le Vaillant, M, Thorne, RL, Aspandiar, M and Verrall, M 2019, Plundering Carlow Castle: first look at a unique Mesoarchean-hosted Cu-Co-Au deposit: *Economic Geology and the Bulletin of the Society of Economic Geologists*, v. 114, no. 6, p. 1021–1031, doi.org/10.5382/econgeo.4672.
- Geological Survey of Western Australia 2020, Northwest Pilbara, 2020: Geological Survey of Western Australia, Geological Information Series, data package (USB).
- Hancock, EA and Beardsmore, TJ 2020, Provenance fingerprinting of gold from the Kurnalpi Goldfield. Geological Survey of Western Australia Report 212, 21p.
- Hickman, AH 2002, Geology of the Roebourne 1:100 000 sheet: Geological Survey of Western Australia, 1:100 000 Geological Series Explanatory Notes, 35p.
- Hickman, AH 2016, Northwest Pilbara Craton: A record of 450 million years in the growth of Archean continental crust: Geological Survey of Western Australia, Report 160, 104p.
- Hickman, AH 2022a, Andover Intrusion (A-OPan-xo-a): Geological Survey of Western Australia, WA Geology Online, Explanatory Notes extract, viewed 11 April 2022, <www.dmirs.wa.gov.au/ens>.
- Hickman, AH 2022b, Ruth Well Formation (A-ROr-xb-u): Geological Survey of Western Australia, WA Geology Online, Explanatory Notes extract, viewed 8 April 2022, <www.dmirs.wa.gov.au/ens>.
- Hickman, AH 2022c, Weerianna Basalt (A-ROw-b): Geological Survey of Western Australia, WA Geology Online, Explanatory Notes extract, viewed 11 April 2022, <www.dmirs.wa.gov.au/ens>.
- Murray, S 2009, LBMA certified reference materials. Gold project final update: The London Bullion Market Association, Alchemist, no. 55, p. 11–12.

## Recommended reference for this publication

- Hancock, EA, Blay, OA and Beardsmore, TJ 2023, 201975: gold grain, Carlow Castle prospect; GSWA Mineralogy Record 9: Geological Survey of Western Australia, 5p.